J Mol Med (2010) 88:597–608
DOI 10.1007/s00109-010-0603-8

ORIGINAL ARTICLES

Lipid rafts are primary mediators of amyloid oxidative attack on plasma membrane

Mariagioia Zampagni · Elisa Evangelisti · Roberta Cascella · Gianfranco Liguri · Matteo Becatti · Anna Pensalfini · Daniela Uberti · Giovanna Cenini · Maurizio Memo · Silvia Bagnoli · Benedetta Nacmias · Sandro Sorbi · Cristina Cecchi

Received: 31 July 2009 / Revised: 10 February 2010 / Accepted: 17 February 2010 / Published online: 10 March 2010

Abstract Increasing evidence indicates that cell surfaces are early interaction sites for Aβ-derived diffusible ligands (ADDLs) and neurons in Alzheimer's disease (AD) pathogenesis. Our previous data showed significant oxidative damage at the plasma membrane in fibroblasts from familial AD patients with enhanced Aβ production. Here, we report that lipid rafts, ordered membrane microdomains, are chronic mediators of Aβ-induced lipid peroxidation in SH-SY5Y human neuroblastoma cells overexpressing amyloid precursor protein (APPwt) and APPV717G genes and in fibroblasts bearing the APPV717I gene mutation. Confocal microscope analysis showed that Aβ-oxidised rafts recruit more ADDLs than corresponding domains in control cells, triggering a further increase in membrane lipid peroxidation and loss of membrane integrity. Moreover, amyloid pickup at the oxidative-damaged domains was prevented by enhanced cholesterol levels, anti-ganglioside (GM1) antibodies, the B subunit of cholera toxin and lipid raft structure alteration. An enhanced structural rigidity of the detergent-resistant domains, isolated from APPwt and APPV717G cells and exposed to ADDLs, indicates a specific perturbation of raft physicochemical features in cells facing increased amyloid assembly at the membrane surface. These data identify lipid rafts as key mediators of oxidative damage as a result of their ability to recruit aggregates to the cell surface.

Keywords Aβ42-GM1 colocalisation · Membrane lipid peroxidation · Lipid raft cholesterol · Amyloid precursor protein · Alzheimer's disease fibroblasts · Alzheimer's disease · Beta-amyloid · Gene expression · Cholesterol

M. Zampagni · E. Evangelisti · R. Cascella · G. Liguri · M. Becatti · A. Pensalfini · C. Cecchi (✉)
Department of Biochemical Sciences, University of Florence,
Viale Morgagni 50,
50134 Florence, Italy
e-mail: cristina.cecchi@unifi.it

G. Liguri · B. Nacmias · S. Sorbi · C. Cecchi
Research Centre on the Molecular Basis of Neurodegeneration,
University of Florence,
Florence, Italy

D. Uberti · G. Cenini · M. Memo
Department of Biomedical Sciences and Biotechnologies,
University of Brescia,
Brescia, Italy

S. Bagnoli · B. Nacmias · S. Sorbi
Department of Neurological and Psychiatric Sciences,
University of Florence,
Florence, Italy

Present Address:
A. Pensalfini
Department of Molecular Biology and Biochemistry,
University of California,
Irvine, CA 92697, USA

Introduction

The deposition of diffuse plaques mainly composed of fibrillar aggregates of β-amyloid (Aβ) peptides in the brain parenchyma is a key event in Alzheimer's disease (AD) pathogenesis [1]. Aβ peptides arise from sequential proteolysis of the transmembrane amyloid precursor protein (APP), a type I membrane protein whose function has not yet been clearly defined. Presently, the overproduction and/or the reduced clearance of Aβ peptides are considered key factors underlying their fibrillar polymerisation. Recent studies have suggested that soluble Aβ oligomers correlate better than plaque load with cognitive impairment and

neuronal dysfunction and may be the principal toxic species of Aβ involved in AD [2, 3].

Increasing evidence suggests that amyloid unstable assemblies, also referred to as Aβ-derived diffusible ligands (ADDLs), interact with cell membranes destroying their ordered structure, eventually leading to membrane permeabilisation [4, 5]. Indeed, cell surfaces can catalyse aggregate nucleation, and self-assembly on the bilayer surface is critical for membrane disruption [6]. Accordingly, we have recently described that amyloid oligomers exogenously added to the culture medium of fibroblasts bearing APPV717I gene mutation, obtained from familial AD (FAD) patients, can readily insert into oxidative-damaged surfaces where the membrane integrity is compromised, resulting in a prompt increase in the production of reactive oxygen species [7]. These data support the rising consensus on the major role of membranes as initial triggers of the biochemical modifications culminating with neuronal death [8].

The plasma membrane displays a complex structure with different regions coexisting in dynamic equilibrium. Among these, detergent-resistant membrane (DRM) fractions including caveolae and lipid rafts are cholesterol- and glycosphingolipid-rich dynamic-ordered microdomains freely diffusible throughout the cell membrane [9]. Lipid rafts contain a variable set of membrane proteins, and their clustering is thought to provide a spatial and temporal meeting point for signalling and trafficking molecules [10, 11]. Recently, lipid rafts have been proposed to function as platforms where neurotoxic oligomers of proteins, including the prion protein and the Aβ peptides, are assembled [12, 13]. Moreover, a study aimed at providing information on the proteins involved in extracellular Aβ internalisation inside primary neuronal cells has suggested a caveolae-independent, raft-mediated mechanism [14]. A recent report highlights a fyn-dependent mechanism as a possible molecular basis of membrane-bound Aβ oligomer recruitment to lipid rafts [15]. However, no clear mechanistic evidence about the relation between the preferential amyloid recruitment and physicochemical modifications of lipid rafts is presently available.

To shed further light on the ability of lipid rafts to recruit ADDLs and on the resulting structural modifications induced by aggregate binding, we carried out a study on human SH-SY5Y neuroblastoma cells stably transfected with wild-type APP gene (APPwt) or 717 valine-to-glycine APP-mutated gene (APPV717G) and on cultured skin fibroblasts from a FAD patient bearing 717 valine-to-isoleucine APP gene mutation (APPV717I). In our model cells, lipid rafts/DRMs are primary sites of Aβ-induced lipid peroxidation and physicochemical perturbation on the cell surface, leading to disruption of selective permeability of plasma membrane. These results identify lipid rafts as specific mediators of oxidative damage and membrane degeneration in neurons with a chronic exposure to increased levels of Aβ42 peptide as a result of their ability to recruit aggregates to the cell surface.

Materials and methods

Materials

All reagents were of analytical grade or highest purity available. Aβ42 peptide as trifluoroacetate salt, cholesterol-water soluble balanced with methyl-β-cyclodextrin (Chol), *N*-[*N*-(3,5-difluorophenacetyl)-L-alanyl]-*S*-phenylglycine *t*-butyl ester (DAPT), 1,6-diphenyl-1,3,5-hexatriene (DPH), foetal bovine serum (FBS), Geneticin (G418), hexafluoro-2-isopropanol (HFIP), mevastatin (Mev), phosphate-buffered saline (PBS) and other chemicals were from Sigma (Milan, Italy) unless otherwise stated. Lyophilised Aβ42 and Aβ42 amine-reactive succinimidyl esters of carboxyfluorescein (Aβ42-FAM, AnaSpec, San Jose, CA, USA) were dissolved in HFIP to 1.0 mM and incubated for 1 h at room temperature to allow complete peptide monomerisation. Then, aliquots of Aβ42 were dissolved in dimethylsulfoxide, incubated in F12 medium to 100 μM at 4°C for 24 h and centrifuged at 14,000×*g* for 10 min. The supernatant, defined as the ADDL preparation, consisted of a fibril-free solution of globular assemblies, as routinely assessed by atomic force microscopy [16].

Cell cultures

Primary fibroblasts bearing the 717 valine-to-isoleucine APP gene mutation (APPV717I) and no APP mutation were obtained, respectively, from skin biopsy of a familial Alzheimer patient with clinical assessment and of an age-matched healthy subject carrying no diagnosis of neurological disorders, according to published guidelines [17]. The local ethical committee approved the study protocol, and written consent was obtained from subjects. The two fibroblast lines were grown in Dulbecco's Modified Eagle's Medium (DMEM), supplemented with 10% FBS and subjected to an equal number of passages (ranging from 16 to 18). Human SH-SY5Y neuroblastoma cells (ATCC, Manassas, VA, USA) were cultured in DMEM/F-12 Ham (1:1), supplemented with 10% FBS, 1.0% glutamine and 1.0% antibiotics and maintained in a 5% CO_2-humidified atmosphere at 37°C. The SY5Y clones overexpressing APPwt and FAD-like mutant APPV717G genes were obtained by transfecting 80% confluent cells with 1 μg/well of the pcDNA-APPwt or with pcDNA-APPV717G constructs, respectively, using LipofectamineTM 2000 reagent (Invitrogen, Milan, Italy). A SY5Y clone trans-

fected with an empty pcDNA vector (SY5Y) was used as control cells. Stable transfected cells were cultured in the presence of 300 μg/ml G418. Immunoblot analysis of APP expression in cell lysates and APP distribution in sucrose gradient fractions were carried out on a 12% (*w*/*v*) SDS/PAGE, blotted onto a polyvinylidene difluoride (PVDF) Immobilio-P Transfer Membrane (Millipore Corporation, Bedford, MA, USA), incubated with 1:1,000 diluted mouse monoclonal 6E10 antibodies (Signet, Dedham, MA, USA) and with 1:5,000 diluted peroxidase-conjugated anti-mouse secondary antibodies (Pierce, Rockford, IL, USA) or with 1:5,000 diluted goat polyclonal sc-1615 antibodies against β-actin (Santa Cruz Biotechnology Inc., Santa Cruz, CA, USA) and with 1:5,000 diluted peroxidase-conjugated anti-goat secondary antibodies (Santa Cruz Biotechnology Inc.). The immunolabelled bands were detected using a Super Signal West Dura (Pierce). In a series of experiments, inhibition of γ-secretase activity was achieved by cell treatment with 100 nM DAPT for 24 h, as previously reported [18]. Human Aβ42 peptide levels were quantified both in cell extracts and in the culture media using an Aβ42 ELISA kit (Invitrogen).

Membrane cholesterol and GM1 modulations

The increase and depletion in membrane cholesterol content were achieved by supplementing SY5Y cell culture media with 200 μg/ml soluble cholesterol (Chol) for 3 h at 37°C or with 10 μM Mev for 48 h at 37°C in the presence of 1% FBS, respectively. Membrane fractions were obtained as previously described [19]. Protein content was measured by the method of Bradford [20]. The amount of cholesterol in membrane fractions and lipid rafts was assessed using an Amplex Red Cholesterol Assay Kit (Molecular Probes, Eugene, OR, USA). The depletion in membrane content of monosialotetrahexosylganglioside (GM1) was achieved by the inhibition of glucosylceramide synthase in cell exposed to 25 μM D-threo-1-phenyl-2-decanoylamino-3-morpholino-1-propanol (PDMP; Matreya, LLC, PA, USA) for 48 h, as previously reported [21]. The GM1 levels were detected onto a PVDF membrane spotted with 2 μg membrane proteins, incubated with 1:500 diluted rabbit polyclonal anti-GM1 antibodies (Calbiochem; EMD Chemicals Inc., Darmstadt, Germany) and with 1:5,000 diluted peroxidase-conjugated anti-rabbit secondary antibodies (Pierce) using a Super Signal West Dura.

Confocal analyses

The aggregate adsorption to the cell surface of neuroblastoma cells exposed to 3.0 μM Aβ42-FAM aggregates for 0, 5, 10, 15, 30, 60 and 180 min was quantified using flow cytometric analysis by a FACSCanto (Beckton Dickinson Biosciences, San Jose, CA, USA), as previously reported [19]. The interaction of Aβ42 aggregates with plasma membranes was also monitored in neuroblastoma cells seeded on glass coverslips and exposed or not to DAPT or PDMP by confocal scanning microscopy. After cell exposure to 1.0 μM ADDLs for 60 min, Aβ aggregates were stained for 60 min with 1:1,000 diluted mouse monoclonal 6E10 antibodies and for 90 min with 1:1,000 diluted Texas Red-conjugated anti-mouse secondary antibodies (Vector Laboratories, DBA, Italy) and plasma membrane profiles for 10 min with 5.0 μg/ml fluorescein-conjugated wheat germ agglutinin (Molecular Probes). In another set of experiments, ADDLs added to cell culture media were detected by incubating cells for 60 min with 1:300 diluted rabbit polyclonal A11 anti-Aβ antibodies (Invitrogen) and for 90 min with 1:1,000 diluted Alexa Fluor 488-conjugated anti-rabbit secondary antibodies (Invitrogen). Plasma membranes were stained with Alexa Fluor 633-conjugated wheat germ agglutinin (Molecular Probes). The colocalisation of Aβ42 aggregates with GM1 was monitored in neuroblastoma cells and fibroblasts seeded on glass coverslips using mouse monoclonal 6E10 antibodies and with 1:1,000 diluted fluorescein-conjugated anti-mouse secondary antibodies (Vector Laboratories) and with 4.5 μg/ml Alexa Fluor 647-conjugated cholera toxin subunit B (CTX-B, Molecular Probes). Cell fluorescence was analysed by a confocal Leica TCS SP5 scanning microscope (Mannheim, Germany) equipped with an argon laser source for fluorescence measurements using excitation lines at 488, 568, 633 and 647 nm for fluorescein, Texas Red, Alexa Fluor 633-conjugated wheat germ agglutinin and Alexa Fluor 647-conjugated CTX-B, respectively. A series of optical sections, (1,024×1,024 pixels) 1.0 μm in thickness, was taken through the cell depth for each examined sample using a Leica Plan Apo 63 × oil immersion objective and projected as a single composite image by superimposition. GM1 colocalisation with Aβ42 aggregates on the cell membrane was estimated on regions of interest (12–13 cells) using the ImageJ (NIH, Bethesda, MD, USA) and JACOP plugin (rsb.info.nih.gov) softwares [22]. For confocal analysis of membrane permeability, neuroblastoma cells were loaded with 2.0 μM calcein-AM (Molecular Probes) for 20 min at 37°C, as previously described [23]. Then, the cells were incubated for 20 min in the absence or in the presence of 4.5 μg/ml Alexa Fluor 647-conjugated CTX-B or 1:100 diluted rabbit polyclonal anti-GM1 antibodies, before treatment with 1.0 μM Aβ42 aggregates for 60 min.

Lipid peroxidation analyses

The levels of 8-OH isoprostane were measured in the cell lysates and raft fractions using the 8-isoprostane EIA kit

(Cayman Chemical Company, Ann Arbor, MI). Total cell lysates were obtained from neuroblastoma cells and fibroblasts, as previously described [16]. Membrane lipid peroxidation was also investigated by confocal microscope analysis of the green (ex 485 nm/em 520 nm) and red signal (ex 581 nm/em 591 nm) of the fluorescent probe BODIPY 581/591 C_{11}, as previously described [19]. Neuroblastoma cells, cultured on glass coverslips, were pre-incubated for 20 min in the absence or in the presence of 4.5 μg/ml Alexa Fluor 647-conjugated CTX-B or 1:100 diluted rabbit polyclonal anti-GM1 antibodies and exposed to 1.0 μM Aβ42 aggregates for 60 min before dye loading. The levels of malondialdehyde (MDA) plus 4-hydroxynonenal (4-HNE) were determined in the raft fractions of neuroblastoma cells using the Aldetect Lipid Peroxidation Assay kit (Enzo Life Sciences Inc, NY, USA).

Purification of DRMs and steady-state fluorescence anisotropy

The cells dispersed in a 10-mM Tris–HCl buffer, pH 7.5, containing 150 mM NaCl, 5.0 mM ethylenediaminetetraacetic acid (EDTA), 1.0 mM Na_3VO_4, 1.0% Triton X-100 (TNE buffer) with protease inhibitors, were disrupted in a Dounce homogeniser and centrifuged at 1,500×*g* for 5 min at 4.0°C, as previously reported [16]. The post-nuclear lysate was adjusted to 40% (*w*/*v*) sucrose by 1:1 addition of 80% sucrose prepared in TNE buffer, placed at the bottom of an ultracentrifuge tube and overlaid with two layers of 30% and 5% sucrose in TNE buffer. The sucrose gradient was centrifuged at 170,000×*g* for 18 h at 4.0°C using a Beckman SW50 rotor. Fractions were then collected from the top of the gradient as follows: 0.5 ml for fraction 1, 0.25 ml for fractions 2 to 11, 1 ml for fractions 12 and 13, while the pellet was dissolved in 0.08 ml of TNE buffer (fraction 14). A representative amount of each fraction was subjected to immunoblot analysis of flotillin-1 on a 12% (*w*/*v*) SDS/PAGE, blotted onto a PVDF membrane, incubated with 1:500 diluted mouse monoclonal primary antibodies (BD Biosciences, San Diego, CA) and anti-mouse secondary antibodies. The flotillin-1-rich fractions were pooled as DRMs and extensively dialysed against TNE buffer to remove sucrose. The amount of sphingomyelin in lipid rafts was assayed using the Sphingomyelin Assay Kit (Cayman Chemical, Ann Arbor, MI, USA). Fluorescence anisotropy (*r*) of DPH was used to measure the structural order of the hydrophobic region of the lipid rafts under steady-state conditions by a Perkin-Elmer LS 55 luminescence spectrometer, as previously reported [16]. Lipid rafts were incubated for 10 min in the absence or in the presence of Aβ42 aggregates at differing concentrations (0.01, 0.1, 1.0 and 10 μM) and then incubated for 30 min with DPH at a 1:250 probe-to-lipid ratio. In another set of experiments, lipid rafts were incubated for 0, 2, 10, 30 and 60 min in the presence of 1.0 μM Aβ42 aggregates before dye loading.

Statistical analysis

All data were expressed as mean ± standard deviation (SD). Comparisons between the different groups were performed by ANOVA followed by Bonferroni's *t* test. A *p* value less than 0.05 was accepted as statistically significant.

Results

Higher lipid peroxidation levels in APPwt and APPV717G overexpressing cells

SH-SY5Y neuroblastoma cells, stably transfected with APPwt and APPV717G constructs, expressed higher APP levels (about threefold) compared to cells transfected with an empty pcDNA vector (Fig. 1a). In particular, APPwt and APPV717G clones showed very similar APP expression levels, providing a useful tool for investigating the dependence of ADDLs binding to neuronal cells on Aβ production level. Indeed, APP undergoes proteolytic β-secretase and γ-secretase activities and generates elevated amounts of Aβ42 peptide both in APPwt and APPV717G neuroblastoma cells and in their culture media (Fig. 1a). However, APPV717G cells produced and released a significant higher level of Aβ42 peptide than APPwt cells. In amyloid diseases, the aggregated species of Aβ peptides interact with the plasma membrane of the affected cells, triggering a free radical-mediated injury that ultimately results in cell degeneration [8, 24]. A confocal microscope analysis showed a higher membrane lipid peroxidation in APPV717G and, to a lesser extent, in APPwt than in SY5Y cells as assessed using the fluorescent probe BODIPY 581/591 (Fig. 1b). By contrast, no difference in the lipid peroxidation levels in the presence of DAPT, a specific γ-secretase inhibitor, was observed among the three clones. These results suggest that the enhanced lipid peroxidation in APP overexpressing clones is predominantly the result of a chronic exposure to increased levels of Aβ42 peptide, rather than to a higher APP content. Accordingly, 8-OH isoprostane levels were significantly higher in APPwt and APPV717G cells compared to SY5Y cells (Fig. 1b), suggesting an oxidative-stressed condition associated with chronic exposure to Aβ in the former. Then, we investigated whether the surface lipid peroxidation enhances the binding process of exogenously added Aβ42 aggregates in APPwt and APPV717G cells. Flow cytometric analysis of the distribution of Aβ42-FAM fluorescent-positive cells showed a curve shift towards higher intensity levels in APPwt and APPV717G cells compared to SY5Y cells

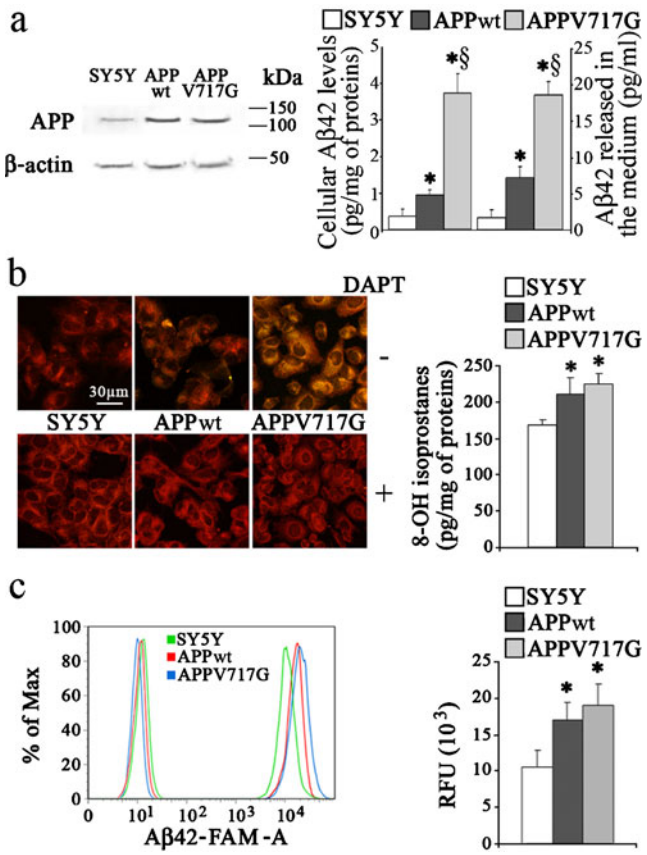

Fig. 1 APPwt and APPV717G overexpressing cells show higher lipid peroxidation levels and attract more Aβ42-FAM aggregates to the plasma membrane. **a** Representative western blot analysis of total extracts from SH-SY5Y neuroblastoma cells overexpressing wild-type APP gene (*APPwt*), FAD-like mutant 717 valine-to-glycine APP gene (*APPV717G*) or mock transfected (*SY5Y*) was carried out using monoclonal mouse 6E10 antibodies. β-Actin expression analysis was used as control loading. Aβ42 levels were measured using a commercial ELISA kit in the cellular extracts and in the conditioned media of the three clones. **b** Representative confocal microscope images of lipid peroxidation in SY5Y, APPwt and APPV717G cells pre-treated or not with 100 nM DAPT for 24 h, as assessed using the fluorescent probe BODIPY 581/591. Lipid peroxidation was quantified by measuring 8-OH isoprostane levels in the three clones. **c** Representative curves and histograms illustrate the flow cytometric analysis of Aβ42-FAM binding to the three clones. The reported values (means ± SD) are representative of three independent experiments carried out in triplicate. * Significant difference ($p \leq 0.05$) vs SY5Y cells. § Significant difference ($p \leq 0.05$) vs APPwt cells

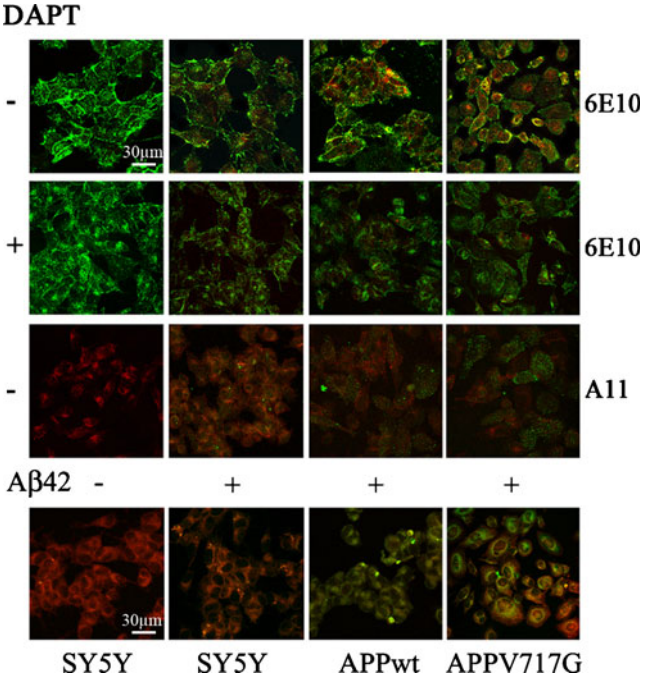

Fig. 2 APPwt and APPV717G overexpressing cells show a greater Aβ42 aggregate recruitment to the plasma membrane. Representative confocal microscope images showing aggregates penetrating into the plasma membrane of SY5Y, APPwt and APPV717G neuroblastoma cells treated with 1.0 μM ADDLs for 60 min (+) compared to untreated cells (−). Cells cultured in the absence (−) or in the presence (+) of 100 nM DAPT for 24 h are compared by labelling Aβ42 aggregates with monoclonal mouse 6E10 antibodies (*red*). The plasma membrane profile was stained with fluorescein-conjugated wheat germ agglutinin (*green*). In the *third set* of images, ADDLs were counterstained using polyclonal rabbit A11 anti-oligomer antibodies (*green*), while the plasma membrane profile was stained with Alexa Fluor 633-conjugated wheat germ agglutinin (*red*). *Bottom*, the fourth set of images was obtained using the fluorescent probe BODIPY 581/591 as a marker of lipid peroxidation in SY5Y, APPwt and APPV717G clones before (−) and after (+) Aβ42 exposure

exposed to ADDLs for 60 min (Fig. 1c). In particular, the mean fluorescent signal of aggregate-binding cells was significantly higher in APP overexpressing clones than in SY5Y clone. Accordingly, confocal microscope analysis showed that when 1.0 μM ADDLs were added to the culture media for 60 min, they accumulate and are internalised mostly in APPwt and APPV717G than in SY5Y cells (Fig. 2). By contrast, DAPT strongly reduced the aggregate binding to plasma membranes of all three clones exposed to ADDLs, excluding the possibility that amyloid pickup at the cell surfaces is merely affected by the APP content. Moreover, an increased aggregate-binding capacity was apparent in APPwt and APPV717G clones compared to SY5Y cells also using A11 antibodies, unable to cross-react with the full-length human APP (Fig. 2). This evidence lets us to rule out the possibility that the differences in 6E10 fluorescence signal were due to different APP expression levels among the three clones. The elevated accumulation of aggregates to the cell surfaces resulted in a sharper increase in membrane oxidative injury as assessed using the fluorescent probe BODIPY 581/591 (Fig. 2). Indeed, APPwt and APPV717G cells showed a significantly higher shift to green fluorescence signal with respect to their respective change in SY5Y cells, when exposed to ADDLs, confirming an enhanced oxidative insult in cellular surface facing a higher Aβ production.

Membrane cholesterol depletion increases Aβ aggregate binding to the cell surface

Then, we investigated the dependence of membrane capacity to bind Aβ42 oligomers on membrane cholesterol content in APPwt and APPV717G clones. In particular, we induced modifications of membrane cholesterol content by incubating neuroblastoma cells in the presence of either water soluble cholesterol (Chol) or Mev. Quantitative analysis showed a significant increase in membrane cholesterol in SY5Y, APPwt and APPV717G cells (17.01±2.8 μg/mg protein, $p \leq 0.05$) after treatment with soluble cholesterol with respect to untreated control cells (12.93±1.52 μg/mg protein). Conversely, clones treated with mevastatin underwent a significant reduction in membrane cholesterol (8.96±0.91 μg/mg protein, $p \leq 0.05$) vs counterpart cells. Anyway, no significant difference was observed in the cholesterol content among these three clones. The increase in cholesterol content resulted in a reduced membrane capacity to bind amyloid aggregates in APPwt and APPV717G clones with respect to corresponding cells, as assessed by confocal microscope analysis of cells exposed to 1.0 μM ADDLs for 60 min (Fig. 3a). To exclude the contribute of intracellular Aβ, a time course of aggregate binding to APPwt and APPV717G cells was also performed by a quantitative flow cytometric analysis of cells exposed to fluorescent Aβ42-FAM aggregates. Cell supplementation with cholesterol resulted in a lower membrane ability to bind Aβ42-FAM. Conversely, ADDLs appeared to accumulate more rapidly and to a greater extent at the plasma membrane in mevastatin treated clones, with a reduced content of cholesterol, than in counterpart cells (Fig. 3a). Moreover, amyloid pickup at the membranes was higher in APPV717G than in APPwt cells. Notably, a slight red fluorescence signal is evident in both the analysed clones without exogenous addition of Aβ42 aggregates, supporting a constant overproduction of Aβ42 in these cells (Fig. 3b). However, APP overexpression could also explain the presence of 6E10 fluorescent signal in the absence of Aβ oligomers [25]. According to the above reported data, a complete absence of red fluorescence signal in the presence of DAPT in both clones occurred (Fig. 3b).

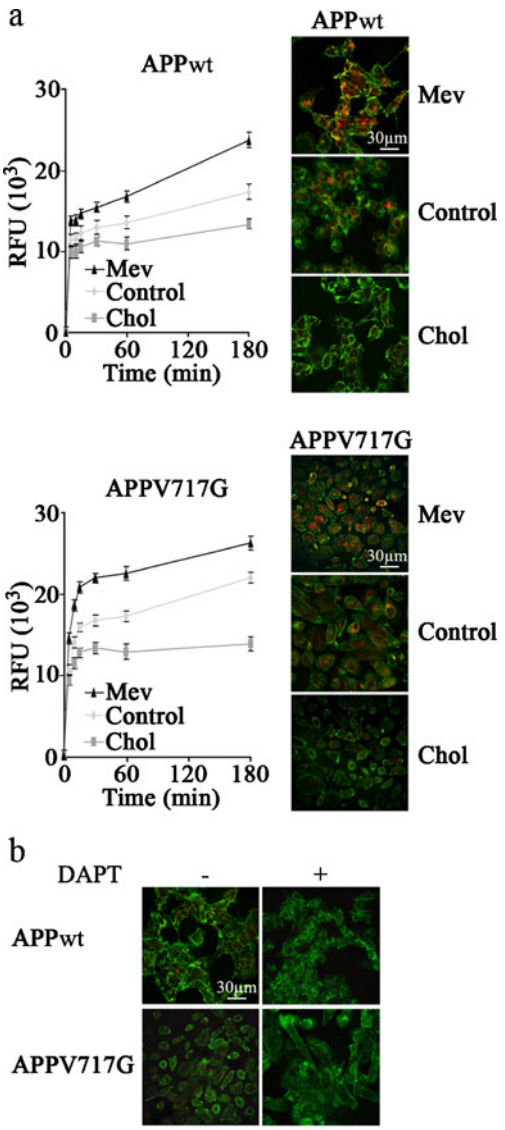

Fig. 3 Membrane cholesterol depletion increases Aβ aggregate binding to APPwt and APPV717G cells. **a** Flow cytometric analysis of Aβ42-FAM binding to the two clones after treatment for differing lengths of time (0, 2, 10, 15, 30, 60 and 180 min) with 3.0 μM Aβ42-FAM aggregates in basal (*Control*), in cholesterol-enriched (*Chol*) and in cholesterol-depleted (*Mev*) conditions. The reported values (mean ± SD) are representative of three independent experiments carried out in duplicate. On the *right*, representative confocal microscope images showing aggregates penetrating into the plasma membrane of APPwt and APPV717G clones after exposure to 1.0 μM Aβ42 aggregates for 60 min, in basal conditions and after treatment with Chol or Mev. **b** Representative confocal microscope images showing APPwt and APPV717G clones cultured in the absence (−) or in the presence (+) of 100 nM DAPT for 24 h. The plasma membrane profile was stained with fluorescein-conjugated wheat germ agglutinin (*green*), and Aβ42 aggregates were labelled with 6E10 antibodies (*red*)

Lipid rafts are primary recruitment sites and oxidative mediators of amyloid aggregates

Recently published research indicates that exogenously applied Aβ in the form of ADDLs can be trafficked on the neuronal membrane and accumulate in lipid rafts, liquid-ordered microdomains rich in cholesterol [14, 15]. Therefore, we investigated the role of cholesterol in the modulation of Aβ42 aggregate interaction with these liquid-ordered structures. Confocal microscope analysis showed a marked colocalisation of Aβ42 oligomers with GM1, a well-known lipid raft marker, on the plasma membranes (Fig. 4a). The analysis of the scatter plots of fluorescence signals using the Pearson's correlation coeffi-

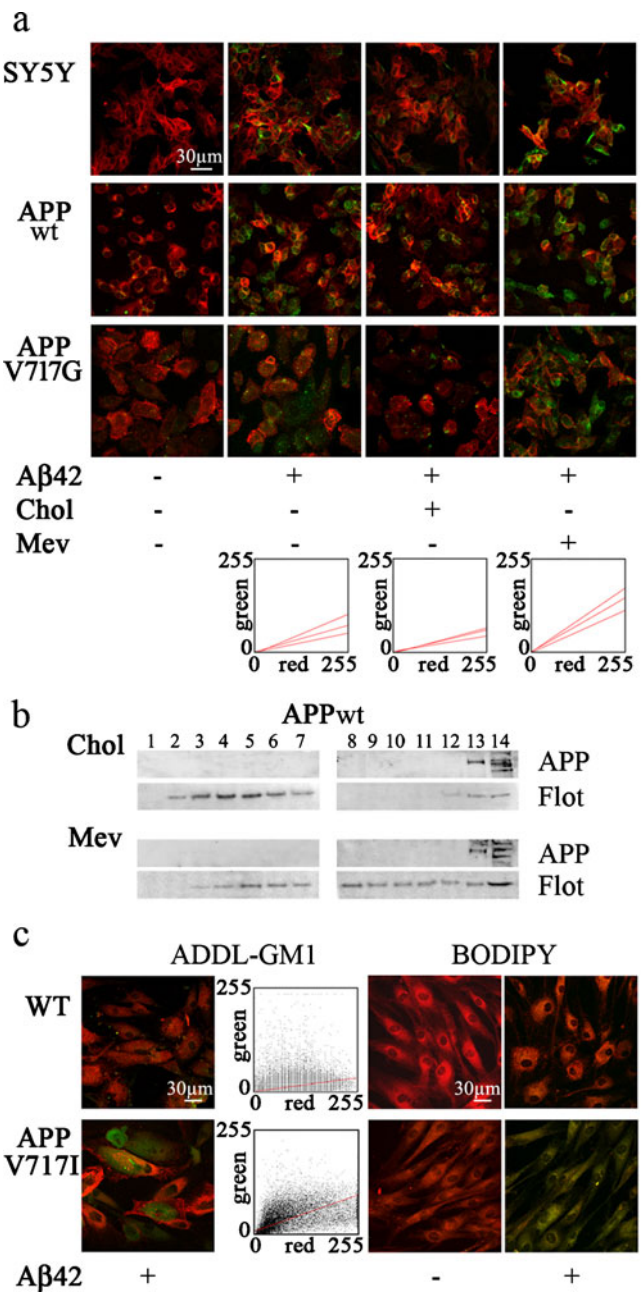

Fig. 4 Aβ42 oligomers preferentially colocalize with the raft domains and generate high-lipid peroxidation in APPV717I fibroblasts. **a** Representative confocal microscope images showing Aβ42-GM1 colocalisation in SY5Y, APPwt and APPV717G cells exposed to 1.0 μM Aβ42 for 60 min in basal conditions and after treatment with Chol or Mev. Aβ42 aggregates were labelled with 6E10 antibodies (*green*), while GM1 was stained with Alexa Fluor 647-conjugate CTX-B (*red*). The scatter plots compare the pattern of Aβ42-GM1 colocalisation in the three clones. The sampled pixels are plotted as a function of *red* (*x*-axis) and *green* (*y*-axis) fluorescence intensity, resulting in partial colocalisation (*left panel*), a low degree of colocalisation (*middle panel*) and a high degree of colocalisation (*right panel*) of Aβ42 aggregates with GM1. **b** Representative immunoblot analyses of APP and flotillin-1 distributions in 14 sucrose gradient fractions of APPwt cells enriched (*Chol*) or depleted (*Mev*) in membrane cholesterol levels. The gradient fractions were collected from the top (low density) to the bottom (high density) of the gradient tube, run on 12% SDS/PAGE and labelled with 6E10 antibodies and mouse anti-flotillin-1 monoclonal antibodies. **c** Representative confocal images showing Aβ42-GM1 colocalisation in wild-type (*WT*) and mutant 717 valine-to-isoleucine APP (*APPV717I*) fibroblasts are shown on the *left-hand side*. ADDLs were labelled with 6E10 antibodies (*green*), while GM1 was stained with Alexa Fluor 647-conjugated CTX-B (*red*). The scatter plots show the pattern of Aβ42-GM1 colocalisation as reported above. Representative confocal microscope images of lipid peroxidation in WT and APPV717I fibroblasts exposed (+) or not (−) to 1.0 μM Aβ42 for 60 min using the fluorescent probe BODIPY 581/591 are shown on the *right-hand side*

cient and the overlap coefficient, according to Manders, yielded a colocalisation of about 51% between GM1 and Aβ42 aggregates in APPwt and APPV717G cells and 42% in SY5Y cells. A moderate enrichment of membrane cholesterol reduced the interaction of ADDLs with GM1 to about 35% colocalisation in APPwt and APPV717G clones and to 25% in SY5Y cells. By contrast, in cholesterol-depleted cells, an increase in ADDL-GM1 colocalisation (about 68%) in APPwt and APPV717G cells and (61%) in SY5Y cells was detected. Then, we investigated whether cholesterol modulation induces an APP redistribution in membrane compartments, accounting for the altered membrane ability to bind amyloid aggregates in APP clones. When APPwt membrane components were separated on a sucrose gradient, no shift in APP immunoreactivity was evident in cholesterol-enriched compared to depleted cells, whereas a flotillin-1 transfer to the higher density fractions in the presence of raft reorganisation occurred (Fig. 4b). Overall, our data showed that Aβ oligomers interact with the plasma membrane preferentially at the raft domains and that any structural modification induced by cholesterol results in alterations of the aggregate–raft interactions. To make these data more relevant, we extended our study to human primary fibroblasts carrying APPV717I gene mutation, obtained from a FAD patient. A higher lipid peroxidation was evident in APPV717I fibroblasts with respect to wild-type fibroblasts obtained from a healthy subject as assessed by the fluorescent BODIPY 581/591 shift (Fig. 4c), suggesting that cells carrying an altered proteolytic APP process have an increased amyloid assembly at the membrane surface. Then, we investigated whether the more oxidised membranes of APPV717I fibroblast bind more exogenous ADDLs at the lipid raft levels. A higher Aβ42-GM1 colocalisation (59%) was evident in APPV717I than in wild-type fibroblasts (40%; Fig. 4c). This resulted in a further increase of membrane lipid peroxidation in mutated fibroblasts, when exposed to ADDLs (Fig. 4c). By contrast, wild-type fibroblasts are more resistant to Aβ-oxidative attack with a slight fluorescence shift, likely because of their plasma membrane integrity.

Oxidative effects of Aβ42 oligomers on detergent-resistant membranes

To confirm Aβ42-specific interaction with lipid rafts, we investigated the biophysical modifications induced by ADDLs in Triton X-100 detergent-resistant membranes (DRMs) isolated from SY5Y, APPwt and APPV717G cells at low temperature. The sucrose gradient fractions rich in flotillin-1 raft marker (fractions from 3 to 5) were pooled and analysed for the 8-OH isoprostane content, MDA plus 4-HNE levels (Fig. 5a, c). A significant higher lipid peroxidation in DRMs from APPwt and APPV717G clones with respect to SY5Y DRMs was evident, whereas no APP redistribution in membrane compartments occurred (Fig. 5a, c). Moreover, a significant higher level of 8-OH isoprostanes in DRMs from APPV717I fibroblasts with respect to wild-type fibroblasts from a healthy subject occurred (Fig. 5b). In particular, the increase in lipid peroxidation levels was higher (about tenfold) in DRM compartments than in the entire membrane, confirming lipid rafts as a preferential site for aggregate binding to cell surface. Then, we evaluated the effect of Aβ42 oligomers on the structural order of the hydrophobic regions of DRMs by measuring the fluorescence anisotropy of DPH dye under steady-state conditions at 37°C. The relative motion of the DPH molecule within the acyl chain space of the lipid bilayer was determined by polarised fluorescence and expressed as *r*, the anisotropy constant, whose value is inversely proportional to the degree of membrane fluidity. DRMs obtained from APPwt cells displayed a dose-dependent anisotropy increase upon exposure to Aβ42 oligomers (Fig. 5c). Then, we investigated whether the APP expression levels influence the DRM disturbing properties of ADDLs. DRMs from APPwt and APPV717G cells showed a higher reduction of fluidity with respect to corresponding rafts from SY5Y cells when exposed to

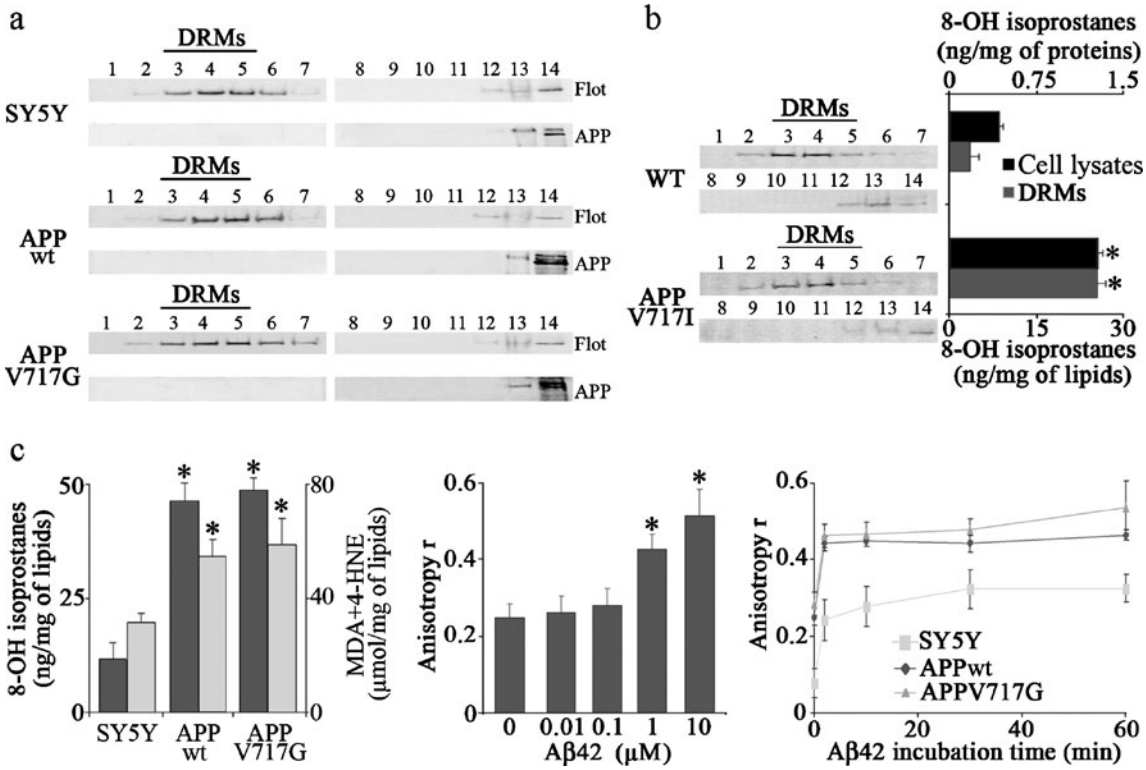

Fig. 5 Oxidative effect of Aβ42 aggregates on DRMs. **a** Representative immunoblot analyses of flotillin-1 and APP distributions in sucrose membrane fractions using specific antibodies as reported above. Flotillin-1-rich fractions (from 3 to 5), consisting of detergent-resistant membranes (*DRMs*), were pooled and extensively dialyzed against TNE buffer to remove sucrose. **b** Representative immunoblot analysis of flotillin-1 levels in sucrose gradient fractions. 8-OH isoprostane levels were quantified both in cell lysates and in pooled flotillin-1-rich fractions (from 3 to 5) consisting of DRMs purified from WT and APPV717I fibroblasts. The reported values (mean ± SD) are representative of three independent experiments carried out in duplicate. * Significant difference ($p \leq 0.05$) vs WT cells. **c** The amount of 8-OH isoprostanes, MDA plus 4-HNE was quantified in DRMs of the three clones. The reported values (mean ± SD) are representative of three independent experiments carried out in triplicate. * Significant difference ($p \leq 0.05$) vs SY5Y cells. DPH fluorescence anisotropy, *r*, was measured by incubating DRMs from APPwt cells with differing concentrations (0.01, 0.1, 1.0 and 10 μM) of ADDLs for 30 min. In another set of experiments, DRMs from SY5Y, APPwt and APPV717G cells were incubated for 0, 2, 10, 30 and 60 min with 1.0 μM Aβ42 aggregates. The reported values (mean ± SD) are representative of six independent experiments, each performed in duplicate. *$p \leq 0.05$, significant difference vs untreated DRMs

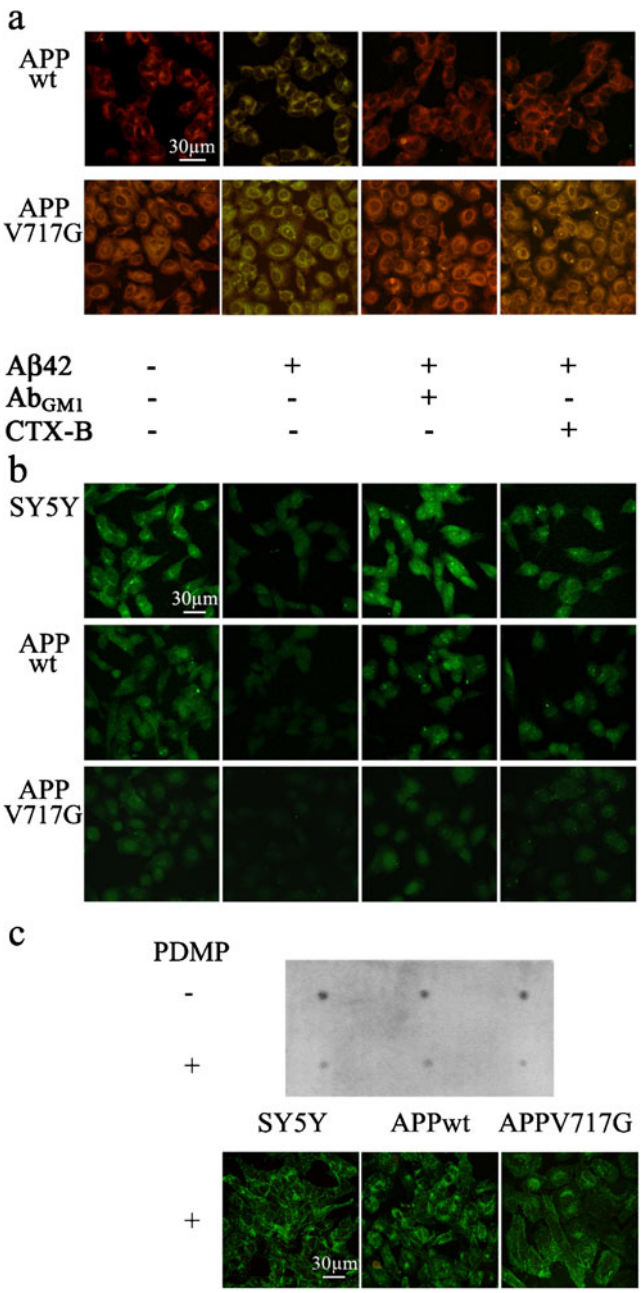

Fig. 6 GM1 mediates accumulation of Aβ42 oligomers on plasma membranes. **a** On the *top*, representative confocal images of lipid peroxidation in APPwt and APPV717G neuroblastoma cells pre-incubated for 20 min with 1:100 diluted rabbit polyclonal anti-GM1 antibodies (Ab_{GM1}) or with 4.5 μg/ml CTX-B and subsequently exposed to Aβ42 aggregates for 60 min as assessed using the fluorescent probe BODIPY581/591. **b** Representative confocal microscope images of SY5Y, APPwt and APPV717G neuroblastoma cells loaded with 2.0 μM calcein-AM for 20 min. The cells were then incubated for 20 min with or without 1:100 diluted rabbit polyclonal anti-GM1 antibodies (Ab_{GM1}) or 4.5 μg/ml CTX-B and subsequently exposed to 1.0 μM ADDLs for 60 min. **c** Representative dot blot analysis of membrane GM1 content in SY5Y, APPwt and APPV717G cells cultured in the absence (−) or in the presence (+) of 25 μM PDMP for 48 h. *Bottom*, representative confocal images of the three clones pre-treated with PDMP and exposed to 1.0 μM Aβ42 aggregates for 60 min. The plasma membrane profile was stained with fluorescein-conjugated wheat germ agglutinin (*green*) and Aβ42 aggregates with 6E10 antibodies (*red*)

ADDLs for different lengths of time (Fig. 5c). Notably, the more ordered structure was reached in less than 10 min of exposure to the oligomers in all cell models. The basal anisotropy level in DRMs from APPwt and APPV717G clones was higher (threefold) than in relatives from SY5Y cells, supporting an increased alteration of membrane structure likely as a result of a chronic exposure to increased levels of Aβ42 peptide.

GM1-mediated accumulation of Aβ42 oligomers on plasma membranes

Previous AFM analysis on DRMs, isolated from SY5Y cells, demonstrated an abundant distribution of GM1 granular structures in these membrane compartments [16]. In order to assess whether lipid rafts are specific mediators of membrane oxidative injury, APPwt and APPV717G cells were pre-incubated with anti-GM1 antibodies (Ab_{GM1}) or with the B subunit of cholera toxin (CTX-B) before exogenously Aβ42 treatment. The specific binding of anti-GM1 antibodies and of CTX-B to raft monosialoganglioside prevented the BODIPY fluorescence shift both in APPwt and APPV717G cells, suggesting a major role of raft domain GM1 in lipid peroxidation process induced by ADDLs (Fig. 6a). Derangement of ion distribution across the plasma membrane is an early biochemical modification displayed by cells exposed to amyloid aggregates [5, 26]. Accordingly, a sharp calcein leakage in SY5Y, APPwt and APPV717G cells was evident (Fig. 6b), suggesting an extensive alteration of membrane permeability induced by Aβ42 aggregates. Moreover, the lower calcein fluorescence in APPwt and APPV717G cells compared to SY5Y cells, before exogenously addition of ADDLs, indicated a chronic amyloid-induced membrane damage in cell facing a higher Aβ production. In order to assess whether raft ability to bind Aβ42 aggregates triggers the loss of membrane integrity, the cells were pre-incubated with anti-GM1 antibodies (Ab_{GM1}) or with CTX-B, and then membrane permeability was analysed in cells exposed to ADDLs. Anti-GM1 antibody and CTX-B binding to GM1 reduced the calcein fluorescence decay (Fig. 6b), supporting a major role of lipid rafts in aggregate recruitment to the cell membrane and in the subsequent alterations of surface properties. To confirm lipid rafts as main targets of Aβ42 incorporation, a specific inhibition of GM1 biosynthesis was achieved in SY5Y APPwt, APPV717G clones using the PDMP (Fig. 6c), while maintaining cell viability (data not shown). The pharmacological interference with lipid raft structure almost prevented Aβ42 incorporation in all clones exposed to ADDLs.

Discussion

Lipid peroxidation is a major outcome of free radical-mediated injury to brain, where it directly damages membranes and generates a number of oxidised products [27]. In the present study, human SH-SY5Y neuroblastoma cells stably expressing about threefold levels of APP and more than threefold levels of Aβ42 showed a higher membrane lipid peroxidation compared to SY5Y control cells, suggesting a chronic oxidative-stressed condition associated with enhanced Aβ production. These findings are in agreement with several studies that provide evidence for excess lipid peroxidation associated with Aβ deposits in APP and PS-1 AD brain and mutant mice [28]. Oxidative damage may further exacerbate Aβ toxicity. Indeed, Aβ is reported to accumulate faster in membranes containing oxidatively damaged phospholipids than in membranes containing only unoxidised or saturated phospholipids [29]. We have previously shown a marked increase in lipid peroxidation levels and an early amyloid binding to oxidative-damaged membranes in fibroblasts from FAD patients [7]. In the present study, a higher membrane oxidative damage resulted in an enhanced ADDL binding to the plasma membrane in neuroblastoma cells over-expressing APPwt and APPV717G as compared to control cells. As recent evidence suggests that Aβ interacts with the APP present at the cell surface and acts as a ligand of its own precursor [30], a minor contribute to Aβ binding could be given by APP overexpression. However, amyloid pick up at the plasma membrane was higher in APPV717G than in APPwt cells, suggesting a causative role for APP mutation in cell surface ability to bind ADDLs. Moreover, DAPT, a specific γ-secretase inhibitor, strongly reduced both the lipid peroxidation levels and the aggregate binding to plasma membranes of all three clones exposed to ADDLs, excluding the possibility that amyloid pickup at the cell surfaces is merely affected by the APP content. Anyway, the early appearance of amyloid aggregates bounded to cell surfaces suggests a main role for these species in oxidative stress process. Indeed, when Aβ42 aggregates were added to cell culture media, they induced a quick membrane lipid peroxidation in APPwt and APPV717G neuroblastoma clones as well as in APPV717I mutated fibroblasts. There is a growing consensus that cell surfaces are patchworks of domains, local concentrations of membrane proteins and lipids quite different from the average for an entire membrane. Cholesterol is likely important in organising some types of domains, usually termed lipid rafts [31]. Increasing data indicate that changes in membrane cholesterol content have regulatory consequences for Aβ interactions with the cell plasma membranes and neurotoxicity [6, 19, 23, 32]. Our confocal and cytofluorimetric evidence on neuroblastoma cells, carrying wild-type and V717G mutated APP, supports this hypothesis. Indeed, when ADDLs were added to the culture medium of cells depleted in membrane cholesterol following treatment with mevastatin, the Aβ42 oligomers appeared to accumulate earlier and to a greater extent at the cell plasma membrane. Recent data suggest that cholesterol depletion, dispersing phosphatidylinositol 4,5-bisphosphate from sites of functional interaction with cell proteins, can alter cell actin organisation and inhibit lateral diffusion of membrane proteins [33]. However, it can be excluded that different APP distribution in plasma membrane compartments, likely resulting from lipid raft reorganisation in our experimental conditions, may contribute to Aβ42 binding to the cell membrane. It has recently been reported that Aβ binding and aggregation occur in lipid raft domains where they are mediated by clusters of the ganglioside GM1 [15, 34]. Our confocal laser microscope analysis showed a marked Aβ42-GM1 colocalisation on membrane rafts in APPV717I-mutated fibroblasts obtained from a FAD patient. Moreover, lipid peroxidation and 8-OH isoprostane quantitative analysis at the raft levels showed that ADDLs induced a more extensive membrane oxidative injury in APPV717I fibroblasts than in control fibroblasts from a healthy subject. These data are also supported by the evidence that lipid composition can influence ADDL recruitment to raft microdomains on neuroblastoma cells. In particular, cholesterol-depleted membranes displayed enhanced ADDL-GM1 colocalisation with respect to control cells, whereas a lower Aβ42 binding to cholesterol-enriched lipid rafts compared to control cells occurred in SY5Y, APPwt and APPV717G cells. Furthermore, the pharmacological interference with lipid raft structure achieved by PDMP, a specific inhibitor of GM1 biosynthesis, prevented Aβ42 incorporation in all clones exposed to ADDLs. Moreover, the anti-GM1 antibody or CTX-B binding to the raft GM1 prevented the amyloid lipid peroxidation process on plasma membrane, suggesting that lipid rafts are specific mediators of membrane oxidative injury in APPwt and APPV717G neuroblastoma cells exposed to Aβ42 aggregates. In addition, a main role of lipid rafts as specific targets of amyloid oxidative damage on plasma membrane cannot be ruled out. Interestingly, membrane lipid peroxidation positively correlates with the perturbing effects of Aβ42 oligomers on DRMs. Indeed, DRMs purified from APP overexpressing cells were more susceptible to the decrease of fluidity produced by ADDL exposure as compared to rafts purified from control cells. As a consequence, APPwt and APPV717G overexpressing cells were more unsuccessful than SY5Y cells in facing aggregate oxidative injury, resulting in a more significant increase in DRM lipid peroxidation. Moreover, the higher increase in lipid peroxidation levels in DRM compartments than in entire

membrane of Alzheimer fibroblasts defines lipid rafts as a preferential site for Aβ aggregate binding to cell surface. These results suggest that the more oxidised the DRMs, the greater its ability to bind specifically ADDLs. Recent evidence suggests that DRMs differ substantially from lipid rafts [35]. Moreover, membrane microdomains can arrange themselves into larger detergent-resistant membrane during triton treatment. Taking into account these limitations, our data are consistent with previous reports indicating that ADDLs affect membrane physical features such as fluidity and density of lipid packing, hindering both membrane oxidation and permeabilisation [9, 10, 13]. Our recent AFM data also showed that treatment of DRMs with ADDLs induced the formation of large steps reflecting differences between the thickness of a standard bilayer and that of a thinner phase [16]. A leading theory on the molecular basis of amyloid toxicity is that pore-like aggregates interact with the cell membranes leading to membrane permeabilisation and free Ca^{2+} imbalance [4, 5, 8]. In the present study, confocal microscope images with the fluorescent probe calcein suggest that DRM disturbing properties of ADDLs were associated to the loss of membrane integrity in SY5Y and APP overexpressing cells. The lower calcein loading in APPwt and APPV717G cells compared to SY5Y cells, before exogenously addition of ADDLs, suggests a chronic amyloid-induced membrane damage with a loss of surface integrity and a constant calcein leakage in cell facing a higher Aβ production. Notably, anti-GM1 antibodies and CTX-B binding to raft GM1 reduced the calcein fluorescence decay induced by ADDLs, supporting a major role of lipid rafts in aggregate recruitment to the cell membrane. This finding suggests that these two ligands can prevent raft structure alteration by decreasing the ADDL binding to GM1 amphipathic targets and subsequently disfavouring Aβ42 incorporation into the membrane. Indeed, the partial lipophilic nature of raft GM1 can account for Aβ42 intracellular uptake. We did not investigate in depth, in our cell system, any direct inhibition of GM1 redistribution by CTX-B and anti-GM1 antibodies. However, the addition of stoichiometric amounts of cholera toxin to samples containing ganglioside GM1 seems to produce only a small decrease in the measured diffusion coefficient [36]. This pattern relies on a progressive amplification mechanism of the early reactive free radicals by repeated chain reaction processes in membrane lipids consistent with the age dependence of AD. These data identify lipid rafts as key mediators of membrane oxidative damage as a result of their ability to recruit Aβ42 aggregates to the cell surface. Finally, an altered APP processing in Alzheimer's fibroblasts strengthens the claim that the changes observed could be the direct outcome of the chronic presence of an increased grade of cellular oxidising environment induced by Aβ.

Acknowledgements The authors would like to thank Daniel Wright for the critical reading of the manuscript. This study has been supported by grants from the Italian MIUR (PRIN project no. 2008R25HBW_002), from the Fondazione Cassa di Risparmio di Pistoia e Pescia (project no. 2009.0202) and Fondazione San Paolo (Alzheimer).

Funding All authors declare the absence of any actual or potential conflicts of interest including any financial, personal or other relationships with other people or organisations within 2 years of beginning the work submitted that could inappropriately influence (bias) their work. All data contained in the manuscript being submitted have not been previously published, have not been submitted elsewhere and will not be submitted elsewhere while under consideration at Journal of Molecular Medicine. All authors have reviewed the contents of the manuscript being submitted, approve of its contents and validate the accuracy of the data.

References

1. Hardy J, Selkoe DJ (2002) The amyloid hypothesis of Alzheimer's disease: progress and problems on the road to therapeutics. Science 297:353–356
2. Walsh DM, Klyubin I, Fadeeva JY, Callen WK, Anvyl R, Wolfe MS, Rowan MJ, Selkoe DJ (2002) Naturally secreted oligomers of amyloid β protein potently inhibit hippocampal long-term potentiation in vivo. Nature 416:535–539
3. Tomic JL, Pensalfini A, Head E, Glabe CG (2009) Soluble fibrillar oligomer levels are elevated in Alzheimer's disease brain and correlate with cognitive dysfunction. Neurobiol Dis 35:352–358
4. Kayed R, Sokolov Y, Edmonds B, McIntire TM, Milton SC, Hall JE, Glabe CG (2004) Permeabilization of lipid bilayers is a common conformation-dependent activity of soluble amyloid oligomers in protein misfolding diseases. J Biol Chem 279:46363–46366
5. Lal R, Lin H, Quist AP (2007) Amyloid beta ion channel: 3D structure and relevance to amyloid channel paradigm. Biochim Biophys Acta 1768:1966–1975
6. Yip CM, McLaurin J (2001) Amyloid-β peptide assembly: a critical step in fibrillogenesis and membrane disruption. Biophys J 80:1359–1371
7. Cecchi C, Fiorillo C, Baglioni S, Pensalfini A, Bagnoli S, Nacmias B, Sorbi S, Nosi D, Relini A, Liguri G (2007) Increased susceptibility to amyloid toxicity in familial Alzheimer's fibroblasts. Neurobiol Aging 28:863–876
8. Stefani M, Dobson CM (2003) Protein aggregation and aggregate toxicity: new insights into protein folding, misfolding diseases and biological evolution. J Mol Med 81:678–699
9. Allen JA, Halverson-Tamboli RA, Rasenick MM (2007) Lipid raft microdomains and neurotransmitter signalling. Nat Neurosci 8:128–140
10. Kusumi A, Suzuki K (2005) Toward understanding the dynamics of membrane raft-based molecular interactions. Biochim Biophys Acta 1746:234–251
11. Yoon IS, Chen E, Busse T, Repetto E, Lakshmana MK, Koo EH, Kang DE (2007) Low-density lipoprotein receptor-related protein promotes amyloid precursor protein trafficking to lipid rafts in the endocytic pathway. FASEB J 21:2742–2752
12. Taylor DR, Hooper NM (2006) The prion protein and lipid rafts. Mol Membr Biol 23:89–99
13. Kim SI, Yi JS, Ko YG (2006) Amyloid beta oligomerization is induced by brain lipid rafts. J Cell Biochem 99:1878–1889

14. Saavedra L, Mohamed A, Ma V, Kar S, Posese de Chaves E (2007) Internalization of β-amyloid peptide by primary neurons in the absence of apolipoprotein E. J Biol Chem 282:35722–35732
15. Williamson R, Usardi A, Hanger DP, Anderton BH (2008) Membrane-bound β-amyloid oligomers are recruited into lipid rafts by a fyn-dependent mechanism. FASEB J 22:1552–1559
16. Cecchi C, Nichino D, Zampagni M, Bernacchioni C, Evangelisti E, Pensalfini A, Liguri G, Gliozzi A, Stefani M, Relini A (2009) A protective role for lipid raft cholesterol against amyloid-induced membrane damage in human neuroblastoma cells. Biochim Biophys Acta 1788:2204–2216
17. The Dementia Study Group of the Italian Neurological Society (2000) Guidelines for the diagnosis of dementia and Alzheimer's disease. Ital J Neurol Sci 21:87–194
18. Wirths O, Thelen KM, Lütjohann D, Falkai P, Bayer TA (2007) Altered cholesterol metabolism in APP695-transfected neuroblastoma cells. Brain Res 1152:209–214
19. Pensalfini A, Zampagni M, Liguri G, Becatti M, Evangelisti E, Fiorillo C, Bagnoli S, Cellini E, Nacmias B, Sorbi S et al (2010) Membrane cholesterol enrichment prevents Abeta-induced oxidative stress in Alzheimer's fibroblasts. Neurobiol Aging (in press)
20. Bradford MM (1976) A rapid and sensitive method for the quantitation of microgram quantities of protein utilizing the principle of protein-dye binding. Anal Biochem 72:248–254
21. Tamboli IY, Prager K, Barth E, Heneka M, Sandhoff K, Walter J (2005) Inhibition of glycosphingolipid biosynthesis reduces secretion of the β-amyloid precursor protein and amyloid β-peptide. J Biol Chem 280:28110–28117
22. Rasband WS (1997–2008) ImageJ. U. S. National Institutes of Health, Bethesda, Maryland. http://rsb.info.nih.gov/ij/
23. Cecchi C, Rosati F, Pensalfini A, Formigli L, Nosi D, Liguri G, Dichiara F, Morello M, Danza G, Pieraccini G et al (2008) Seladin-1/DHCR24 protects neuroblastoma cells against Aβ toxicity by increasing membrane cholesterol content. J Cell Mol Med 12:1990–2002
24. Butterfield DA, Reed T, Newman SF, Sultana R (2007) Roles of amyloid beta-peptide-associated oxidative stress and brain protein modifications in the pathogenesis of Alzheimer's disease and mild cognitive impairment. Free Radic Biol Med 43:658–677
25. Tampellini D, Magrané J, Takahashi RH, Li F, Lin MT, Almeida CG, Gouras GK (2007) Internalized antibodies to the Abeta domain of APP reduce neuronal Abeta and protect against synaptic alterations. J Biol Chem 282:18895–18906
26. Demuro A, Mina E, Kayed R, Milton S, Parker I, Glabe CG (2005) Calcium dysregulation and membrane disruption as a ubiquitous neurotoxic mechanism of soluble amyloid oligomers. J Biol Chem 280:17294–17300
27. Montine KS, Quinn JF, Zhang J, Fessel JP, Robert LJ II, Morrow JD, Montine TJ (2004) Isoprostanes and related products of lipid peroxidation in neurodegenerative diseases. Chem Phys Lipids 128:117–124
28. Abdul HM, Sultana R, St Clair DK, Markesbery WR, Butterfield DA (2008) Oxidative damage in brain from human mutant APP/PS-1 double knock-in mice as a function of age. Free Radic Biol Med 45:1420–1425
29. Murray IV, Liu L, Komatsu H, Uryu K, Xiao G, Lawson JA, Axelsen PH (2007) Membrane-mediated amyloidogenesis and the promotion of oxidative lipid damage by amyloid beta proteins. J Biol Chem 282:9335–9345
30. Shaked GM, Kummer MP, Lu DC, Galvan V, Bredesen DE, Koo EH (2006) Abeta induces cell death by direct interaction with its cognate extracellular domain on APP (APP 597–624). FASEB J 20:1254–1256
31. Simons K, Toomre D (2000) Lipid rafts and signal transduction. Nat Rev Mol Cell Biol 1:31–39
32. Arispe N, Doh M (2002) Plasma membrane cholesterol controls the cytotoxicity of Alzheimer's disease Abeta (1–40) and (1–42) peptides. FASEB J 16:1526–1536
33. Kwik J, Boyle S, Fooksman D, Margolis L, Sheetz MP, Edidin M (2003) Membrane cholesterol, lateral mobility, and the phosphatidylinositol 4, 5-bisphosphate-dependent organization of cell actin. Proc Natl Acad Sci USA 100:13964–13969
34. Fujita A, Cheng J, Hirakawa M, Furukawa K, Kusunoki S, Fujimoto T (2007) Gangliosides GM1 and GM3 in the living cell membrane form clusters susceptible to cholesterol depletion and chilling. Mol Biol Cell 18:2112–2122
35. Lichtenberg D, Goñi FM, Heerklotz H (2005) Detergent-resistant membranes should not be identified with membrane rafts. Trends Biochem Sci 30:430–436
36. Goins B, Masserini M, Barisas BG, Freire E (1986) Lateral diffusion of ganglioside GMl in phospholipid bilayer membranes. Biophys J 9:849–856